

CHARACTERIZATION, ANTIMICROBIAL, AND METABOLIC ACTIVITY OF GREEN AND CHEMICALLY SYNTHESIZED ZINC OXIDE NANOPARTICLES

SUMATHI S*, BANUPRIYA SJS, AKHILA V, PADMA PR

Department of Biochemistry, Biotechnology and Bioinformatics, Avinashilingam Institute for Home Science and Higher Education for Women, Coimbatore, Tamil Nadu, India. Email: sumii.venkat@gmail.com

Received: 08 July 2019, Revised and Accepted: 09 September 2019

ABSTRACT

Objectives: The aim of the present study is to synthesize zinc oxide nanoparticles (ZnONPs) by green and chemical method. The nanoparticles were tested for their antimicrobial, antibiofilm activity, biocompatibility, and hemolysis activity.

Methods: We have synthesized ZnONPs both by green and chemical synthesis using the coprecipitation method. To understand the functional group, absorbance, crystalline nature, size, and shape of the synthesized particles, Fourier transform infrared (FTIR), ultraviolet-visible spectroscopy, X-ray diffraction, and scanning electron microscopy were done. Antibacterial activity was carried out using different bacterial strains. The cytotoxicity of synthesized nanoparticles was checked using MTT assay with *Klebsiella pneumoniae*. Antibiofilm activities of both synthesized nanoparticles were done using *Staphylococcus aureus* and to assess the toxicity of nanoparticles at the cellular level, hemolysis assay was performed.

Results: The yield of nanoparticles in green synthesis was much higher when compared to chemical synthesis. Spectral results showed that the synthesized nanoparticles were ZnONPs. Antibacterial, antibiofilm, and hemolysis assay showed that green nanoparticles were more potent than chemical nanoparticles.

Conclusion: Hence, green synthesis provides an advantage over chemical synthesis as it is cost effective, environmentally friendly, and easily scaled up for large-scale synthesis.

Keywords: Green nanotechnology, Coprecipitation, Zinc oxide nanoparticles, Characterization, Antibacterial, Antibiofilm, and Hemolysis.

© 2019 The Authors. Published by Innovare Academic Sciences Pvt Ltd. This is an open access article under the CC BY license (<http://creativecommons.org/licenses/by/4.0/>) DOI: <http://dx.doi.org/10.22159/ajpcr.2019.v12i11.34819>

INTRODUCTION

In recent years, nanoparticles are the most thought provoking and fascinating disputes of science and technology in the examination point of understanding due to its unique, optical, electrical, photochemical, and photocatalytic properties. It has diverse innovative applications that range from innovative food processing, agricultural production, and fabric compounds to superior medical techniques [1]. Compared to bulk materials, nanomaterials are beneficial based on the properties they own. The best known materials that have been broadly used for medical applications are zinc oxide nanoparticles (ZnONPs). It is a magical material due to its widespread applications and flexibility of research in different morphologies with different properties [2].

Different methods are used to synthesize nanoparticles such as polyol process, hydrothermal, sol-gel, microemulsion techniques, and coprecipitation method. Among all coprecipitations are the best method because it is simple and economical [1].

Synthesis of nanoparticles using green nanotechnology is an identical and promising area because the plant itself can act as both reducing and capping agent. Medicinal plants are a rich source of a variety of biologically active compounds with antioxidant potentials which can mitigate reactive oxygen species, generated by normal physiological processes and various exogenous factors. *Annona muricata* (Fig. 1) species commonly known as "custard apple" belongs to the family *Annonaceae* is naturally occurring in Central America and southern parts of India. It is described as "the Cancer killer." It is used to treat Alzheimer's disease, Parkinson's disease, reduce oxidative stress, and antivenom activity and has anticancer activity too [3].

The microbial biofilm is widely exploited in the investigation of biology and regulatory mechanism. *In vivo* and *in vitro* methods are used

to measure the formation, maturation, and dispersion of biofilms. For developing new drugs and wound management protocols, the antibiofilm drug discovery is very much essential [4].

METHODS

Collection of samples

The leaf samples of *A. muricata* were collected from Thondamuthur, Coimbatore. The bacterial strains were collected from Microbiological Laboratory, Coimbatore.

Preparation of leaf extract

The leaf samples collected were thoroughly washed using double distilled water, ground, and filtered using Whatman No:1 filter paper and the extract was stored for further process.

Authentication of the plant

The plant specimen (leaf) *A. muricata* L. was identified and authenticated by the Botanical Survey of India, Coimbatore, and the certified number was BSI/SRC/5/23/2019/Tech/186.

Green synthesis of ZnONPs

0.02 M aqueous zinc acetate dihydrate was prepared and aqueous leaf extract of *A. muricata* was introduced to it. pH was adjusted to 12 using 2.0 M NaOH and placed in magnetic stirrer for 2 h. The precipitate was then taken out and washed with distilled water followed by ethanol to get free of impurities. Then, the white powder of ZnONPs was obtained after drying at 60°C in hot air oven overnight.

Chemical synthesis of ZnONPs

0.02 M aqueous zinc acetate dihydrate was prepared and 2.0 M NaOH was added that resulted in a white aqueous solution and then placed

in a magnetic stirrer for 2 h. The white precipitate was then taken out and washed with distilled water followed by ethanol to get free of impurities. Then, a white powder of ZnONPs was obtained after drying at 60°C in hot air oven overnight.

Antimicrobial assay was done using agar well diffusion method by Perez *et al.* (1990) [5], MTT assay by Igarashi and Miyazawa (2001) [6], antibiofilm was tested by the method Christensen *et al.* (1985) [7], and biocompatibility was tested using hemolysis assay as per Gleibs *et al.* (1995) [8].

RESULTS AND DISCUSSION

Synthesis of ZnONPs

ZnONPs were synthesized by coprecipitation method for both green and chemical synthesis. In case of green synthesis, the formation of pale yellow color precipitate after overnight incubation was the primary indicator of the probable synthesis of ZnONPs by the reduction of Zn²⁺ metal ions by the organic reducible agents present with the plant material. Colorless solution changes to a white precipitate formation that confirms the synthesis of ZnONPs by chemical method as shown in (Fig. 2).

Particles size and morphology characterization of ZnONPs

Characterization of nanoparticles is a very important step to identify the structure, shape, and charge of the synthesized nanoparticles. This was supported by considering various parameters such as ultraviolet (UV)-visible spectroscopy, X-ray diffraction (XRD), Fourier transform infrared (FTIR), and scanning electron microscopy (SEM) with EDAX.

UV-visible spectroscopy analysis

The size of the nanoparticles plays an important role in shifting the total properties of a material and it is necessary to investigate the properties of the material. To examine the optical property of the nanosized particles, the widely used technique is UV-visible spectroscopy. Once

the nanoparticles were synthesized by green and chemical methods; it was analyzed using UV-visible spectroscopy to investigate the optical properties of the synthesized particles. The absorption spectrum of ZnONPs ranges from 350 nm to 385 nm.

The results of UV absorption showed characteristic peaks at 355 nm and 380 nm (Fig. 3) correspond to synthesized ZnONPs by green and chemical method, respectively. The peak was observed due to the surface plasmon vibration. Confirmation of the synthesized ZnO product in nanoscale exhibited by the shift in absorption from a bulk ZnONP which is usually around 385 nm. The absorption spectrum of biosynthesized ZnONPs showed a peak around 376 nm due to their large exciting binding energy [9]. Several reports are available confirming our results. Green tea mediated synthesis of ZnONPs showed the absorption range at 325 nm and a peak confirms the blueshift in the absorption spectrum [10]. Zinc oxide nanopowder showed the absorption spectrum at 355 nm and the excitonic absorption peak was found at 258 nm due to the position of the nanoparticles which lie just below the bandgap wavelength of 358 nm [11]. Large assortment of absorption value was observed at 352 nm for chemically synthesized ZnONPs [12].

Our findings are in line with the studies reported as above, confirming the fact that the UV-visible spectrum can be analyzed to confirm the formation of nanoparticles.

FTIR spectroscopy

In FTIR spectroscopy, the absorption of infrared (IR) radiation by a sample plotted against the wavelength was measured. From the spectrum, the biomolecules present in the plant extracts responsible for stabilization and reduction of green synthesis of nanoparticles can be identified. The organic functional group provides an absorption peak at a specific narrow frequency range. The synthesized green and chemical nanoparticles were subjected to FTIR analysis to detect the characteristic functional groups based on the peak value.

The major absorption band spectra of green synthesized ZnONPs were seen at 704 cm⁻¹, 908 cm⁻¹, 1394 cm⁻¹, 1614 cm⁻¹, 3026 cm⁻¹, and 3281 cm⁻¹. Chemically synthesized nanoparticles showed absorption peaks at 765 cm⁻¹, 1101 cm⁻¹, 1350 cm⁻¹, 1525 cm⁻¹, 1631 cm⁻¹, 2358 cm⁻¹, and 3446 cm⁻¹ as shown in Fig. 4. The absorption peaks at 704 cm⁻¹ indicate aromatic C-H, 908 cm⁻¹ shows the presence of aromatic stretching, and 1614 cm⁻¹ shows the presence of C=C stretch in the aromatic ring and C=O stretch in polyphenols. Broad IR bands at 3026 cm⁻¹ and 3281 cm⁻¹ show the presence of hydroxyl group, aldehydes, and amines and 540–417 cm⁻¹ show the stretching vibration of ZnONPs. The absorption peak at 765 cm⁻¹ indicates that C-H bending, 1101 cm⁻¹ band shows that O-C stretching, 1350 cm⁻¹ indicates CH₂ bending, and 1525 cm⁻¹, 1631 cm⁻¹, and 2358 cm⁻¹ which are the characteristic of C=O vibration, C=O stretching in the carboxyl group, and C=O stretching. The deep peak at 3446 cm⁻¹ corresponds to the stretching vibration of the intermolecular hydrogen bond (O-H) existing between the absorbed water molecules and indicates the higher amount of hydroxyl group.

FTIR pattern of ZnONPs ranges from 450 to 4000 cm⁻¹ that absorption frequency at 528 cm⁻¹ and 3451, 1552, 2170, and 1399 cm⁻¹ which correspond to the -OH, N-H, C=C, and C-H bond stretching which indicates the presence of a reduction of ZnONPs [13]. The FTIR spectrum of both chemical and biosynthesized *Pithecellobium dulce* and *Lagenaria siceraria* leaf extract showed strong absorption bands at 2848, 2854, and 2863 cm⁻¹ which may be attributed to the stretching mode of C-H bonds and bonds at 1618, 1622, and 1643 cm⁻¹ are attributed to C=C stretch and C=O vibration [14]. The absorption spectra for Rasagiline mesylate, Stearic acid, and mixtures of Rasagiline mesylate and Stearic acid were found at 2674 cm⁻¹, 1463 cm⁻¹, 2934 cm⁻¹, 2805 cm⁻¹, 3219 cm⁻¹, and 1192 cm⁻¹ which correspond to carboxylic O-H group, CH bending, aromatic C-H stretching, aliphatic CH stretching, secondary amine N-H, and aliphatic amine C-N, respectively [15].



Fig. 1: *Annona muricata*

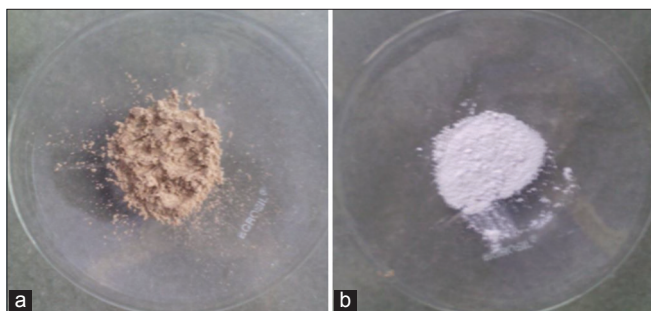


Fig. 2: Synthesis of zinc oxide nanoparticles (a) green synthesis (b) chemical synthesis

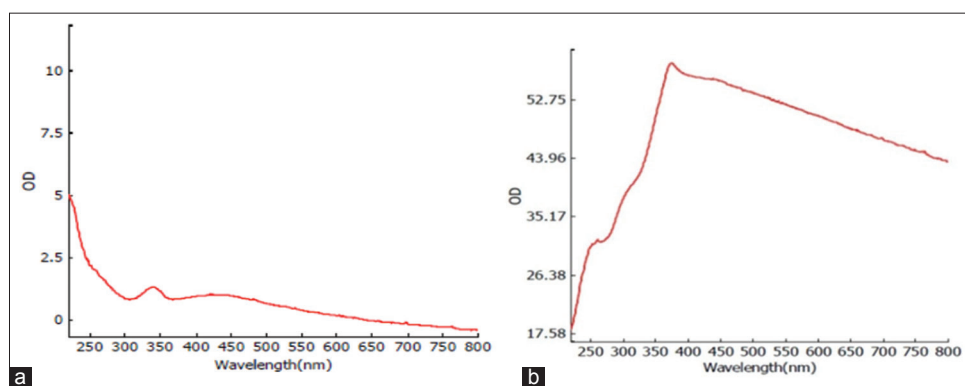


Fig. 3: (a and b) Ultraviolet-visible spectroscopy

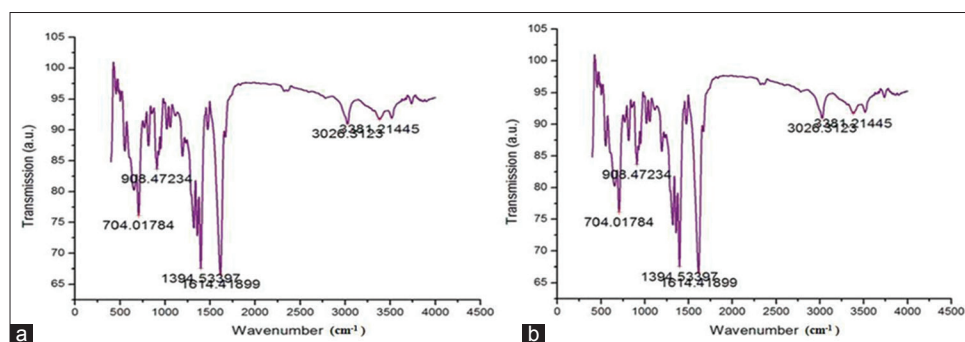


Fig. 4: (a and b) Fourier-transform infrared spectroscopy

Similar kinds of peaks were observed in the present study and proved the presence of ZnONPs which are in accordance with earlier reports.

SEM

The structure, shape, and size of the synthesized ZnONPs were analyzed by SEM. To analyze the structural morphology of the ZnONPs using the powdered form of nanoparticles, SEM was carried out.

Fig. 5 shows that biosynthesized ZnONPs were rod shaped and chemically synthesized ZnONPs were spongy and porous. The morphology was observed under different magnifying ranges. The results of the present study showed that the ZnONPs were loosely arranged and the particles were monodispersed. The size of the ZnONPs under SEM was 100–190 nm. There was no aggregation of particles in the ZnONPs and they were dispersed finely. This reveals the stability of the particles.

Synthesized ZnONPs were found in the range of 30–50 nm and the shape of the nanoparticles was the small spherical shape and was well crystallized [11]. ZnONPs showed individual zinc particles as well as a number of aggregates. The agglomeration is due to polarity and electrostatic attraction of nanoparticles. The SEM image showed the relatively spherical shape formed within the diameter range nm [14]. ZnONPs synthesized by both chemical and green synthesis method showed spherical shape under the SEM [16]. Nanoparticles under low magnification showed the hierarchically nanostructured flowers and flakes ranging from 0.2 μm to 2 μm in diameter. Closer observations have shown flower morphology ranging from 100 nm to 200 nm [17]. The cephalixin-CSNPs nanocomposite appeared as an agglomerated structure with non-uniform size under SEM. This result showed that between nanoparticles there was a strong inter- and intra-molecular hydrogen bonding [18].

Hence, our results are also in accordance with the above findings and confirm the shape and size of the nanoparticles.

XRD

The crystalline nature of the ZnONPs and the phase identification was analyzed using XRD technique. The peak in the diffractogram indicates

that the particles synthesized were crystalline in nature. The powder XRD was carried out to identify the nature of the nanoparticles.

Fig. 6 shows the typical pattern of ZnONPs prepared by green synthesis method and chemically synthesized ZnONPs were crystalline in nature. XRD pattern of synthesized ZnONPs by green method showed strong diffraction peaks with 2θ values of 31.2° , 35.8° , and 39.7° which correspond to the crystal planes of (100), (002), (101), (102), (110), (103), (200), (112), and (201) of crystalline ZnONPs, respectively, and chemical method with 2θ values of 31.2° , 35.8° , 39.1° , 54.1° , and 57.4° which correspond to the crystal planes of (100), (002), (101), (102), (110), (103), (112), and (201). This confirms the presence of ZnONPs.

Similar studies were reported by other researchers. ZnONPs from *Pyrus pyrifolia* leaf extract showed the peaks at (101), (102), (110), (103), (112), and (202) [9]. The absorption spectra for prepared and calcined ZnO nanoparticles were absorbed at (100), (002), (101), (102), (110), (103) and (112) and this confirmed the hexagonal wurtzite structure of the ZnO nanoparticles [10]. Various diffraction peaks were observed at (100), (002), (010), (102), (110), (103), (112), (201), (004), (202), and (104) by the synthesized ZnONPs using a chemical method [11]. The peaks of diffractogram of both biological *Pithecellobium dulce* and *Lagenaria siceraria* Leaf extract and chemically synthesized ZnO nanoparticles were observed at (101), (102), (110), (103) and (112) [14]. The diffraction peaks of synthesized nanoparticles match exactly with the XRD standard data of parent (bulk) which confirms the crystal nature of the ZnONPs. The diffraction pattern for synthesized ZnONPs was attained at (100), (002), (101), (102), (110), (103), (200), (112), (201), and (004) [12]. The results showed that the synthesized nanoparticles were crystalline in nature.

Assessment of biological and biocompatibility of nanoparticle

Antibacterial activity

The antibacterial and biocompatibility of the particles were tested. Biosynthesized ZnONPs were analyzed for their antibacterial activity against Gram-positive bacteria, *Escherichia coli* and *Bacillus subtilis*

and Gram-negative bacteria, *Pseudomonas aeruginosa* and *Klebsiella pneumoniae* by well diffusion method. The well diffusion technique was utilized to compare the antibacterial activity using the synthesized ZnONPs. In this study, 25 µg/ml of ZnONPs was taken to check its antibacterial activity.

Antibacterial activity results revealed that green synthesized nanoparticles have more antibacterial activity against Gram-positive and Gram-negative bacteria, compared to chemically synthesized ZnONPs. The zone was formed around the area where nanoparticles diffused from the wells and it was formed due to toxic effects of the nanoparticles indicative of the fact, they can also act as antibiotics. The zone of inhibition exhibited by nanoparticles against several bacteria tested is shown in Fig. 7. The zone of inhibition by green nanoparticles for *B. subtilis* was found to be highest 22 mm compared to the chemically synthesized nanoparticles which were 17 mm and the maximum inhibition was observed for this organism compared to the other bacterial strains.

The inhibitory response of the ZnONPs was observed against bacterial strains such as *E. coli*, *Staphylococcus aureus*, *Pseudomonas sp.*, *Salmonella sp.*, and *Bacillus sp.* [19]. The highest antimicrobial activity was observed against *P. aeruginosa* compared to other bacterial strains [20]. The presence of inhibition zone clearly indicates that the mechanism of the biocidal action of ZnONPs which involves disruption of the membrane with high rate of generation of surface oxygen species and finally leads to the death of pathogens [21]. Chloramphenicol

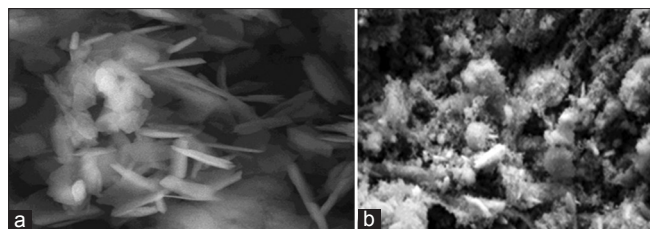


Fig. 5: (a and b) Scanning electron microscopy

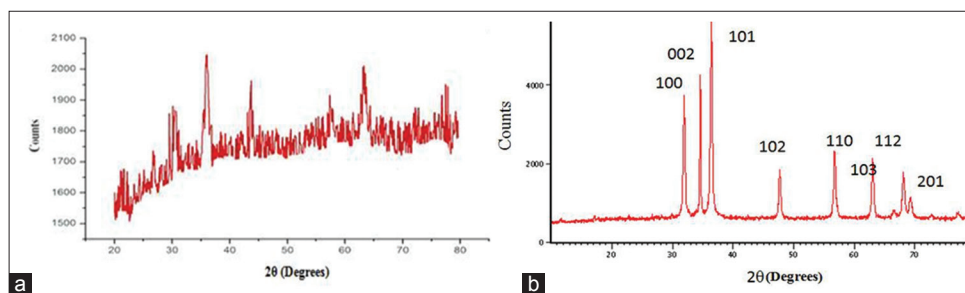


Fig. 6: (a and b) X-ray diffraction analysis of zinc oxide nanoparticles

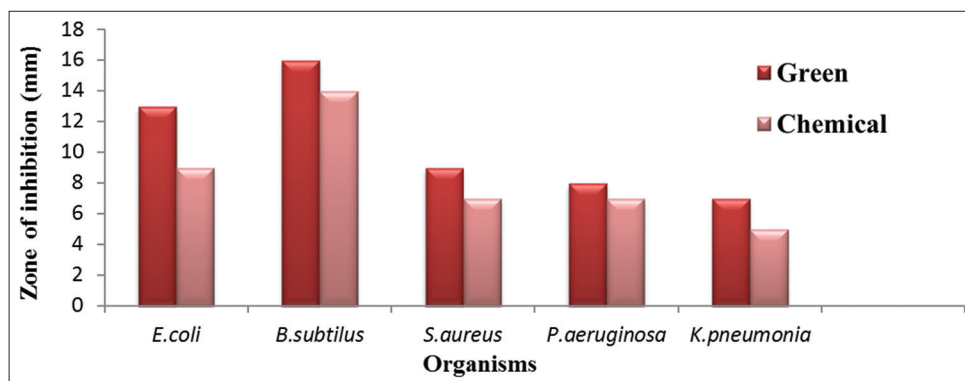


Fig. 7: Antibacterial activity of synthesized zinc oxide nanoparticles

and cephalothin were used as standard reference for Gram-negative and Gram-positive bacteria, respectively. These compounds had very low activity against the Gram-positive bacteria and more activity against the Gram-negative bacteria [22]. Chitosan nanoparticles and cephalixin-loaded chitosan nanoparticles showed very good activity against Gram-positive and Gram-negative bacteria. Comparatively, cephalixin-loaded chitosan nanoparticles showed superior activity than the chitosan nanoparticles [18]. ZnONPs were examined against Gram-positive and Gram-negative bacteria and they were more active against the both [23].

Antimicrobial activity by MTT assay

Antimicrobial activity of nanoparticles is known to be a function of the surface area in contact with the microorganisms. The ions released by the nanoparticles may attach to the negatively charged bacterial cell wall and rupture it thereby leading to protein denaturation and cell death.

For determining the intracellular activity of the cell, cell proliferation, and the cell viability, the MTT assay was done. From the present study, it was clear that as the concentration of nanoparticles increased, the percentage of dead cells also increased as assessed by MTT assay. This was done using the bacterial strain *K. pneumoniae* where different concentrations of the nanoparticles were tested for their inhibitory potential of the microbial growth and hence its viability. The chemically synthesized nanoparticles showed more toxicity compared to green synthesized ZnONPs.

The results of MTT assay as shown in Fig. 8 clearly show that the chemically synthesized ZnONPs at a concentration of 10 µg/ml showed cytotoxicity, whereas minimal cytotoxicity was observed for green synthesized nanoparticles. The percentage of dead cells was increased by increasing the concentration of nanoparticles. Chemically synthesized nanoparticles were more toxic compared to green nanoparticles. The percentage of dead cells reaches 68.5% at 100 µg.

In all incubation times, the highest cell death was observed at a concentration of 1000 µg/ml and the lowest one at 10 µg/ml [24].

ZnONPs demonstrated stronger cytotoxicity against colon HT-2 cancer cells than breast cancer cell lines MCF7 [25]. Antimicrobial activity of iron oxide nanoparticles on *S. aureus* showed better activity [26]. ZnONPs showed better cytotoxic activity against human breast cancer cell line when compared to normal cell line. ZnONPs inhibited the growth of cancer in a dose-dependent manner [27]. ZnONPs were treated with different types of cancer cells (MCF-7, HepG2, and A549) with different concentrations of synthesized ZnONPs. The results showed that the viability of the cells decreased on increasing the concentration of the synthesized ZnONPs [28].

Antibiofilm activity

Microbial biofilms can be defined as a surface-attached community of microorganisms embedded and growing in a self-produced matrix of extracellular polymeric substances. The nanoparticles having antibacterial activity will also exhibit the antibiofilm activity. Antibiofilm effect of green and chemically synthesized nanoparticles against biofilm of *S. aureus* was studied. The microscopic studies

showed well-developed biofilm formation, whereas the treatment with ZnONPs inhibited biofilm formation in a dose- and time-dependent manner. Fig. 9 shows the results of antibiofilm assay. It showed that as the concentration of nanoparticles increased, the antibiofilm activity also increased and it inhibited the biofilm formation. The results showed in Fig. 9 revealed that the chemically synthesized ZnONPs showed maximum inhibition of activity at 72 h. Green synthesized nanoparticles inhibited the growth at 12 h and maximum inhibition was noticed at 72 h which were nearly 100%. The ions released by the nanoparticles may attach to the negatively charged bacterial cell wall and rupture it thereby leading to protein denaturation and cell death.

There was an inhibition of biofilm formation of all the tested bacteria by the free and antibiotics incorporated ZnONPs [4]. The biofilm formation activity of *Streptococcus mitis* ATCC 6249 and Ora-20 on the surface of polystyrene plates was inhibited by both the nanoparticles of zinc oxide and titanium oxide in a concentration-dependent manner [29]. The bacterial strains *P. aeruginosa* and *S. aureus* are known to form

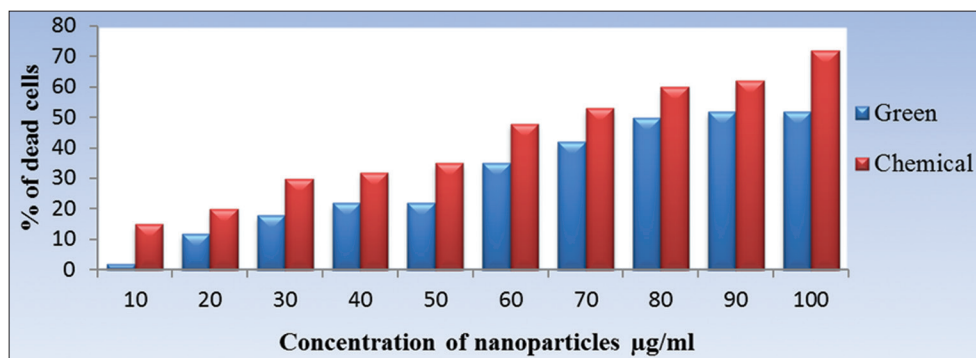


Fig. 8: Antimicrobial activity of zinc oxide nanoparticles by MTT assay

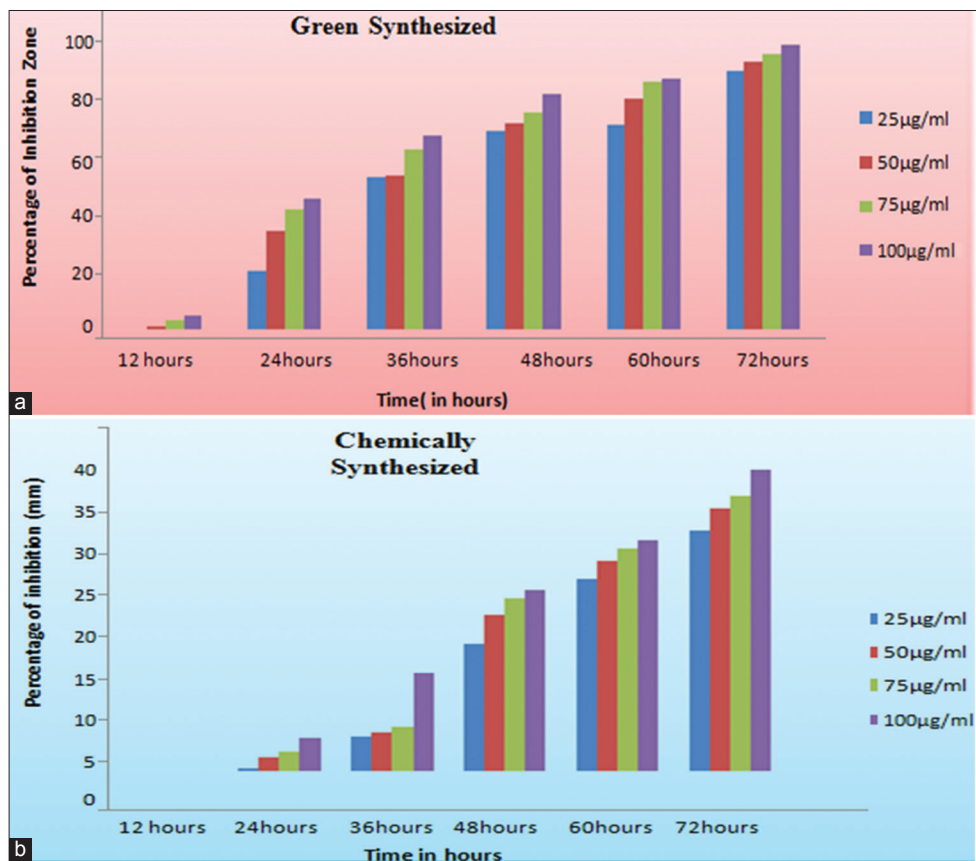


Fig. 9: (a and b) Antibiofilm activity of synthesized nanoparticles

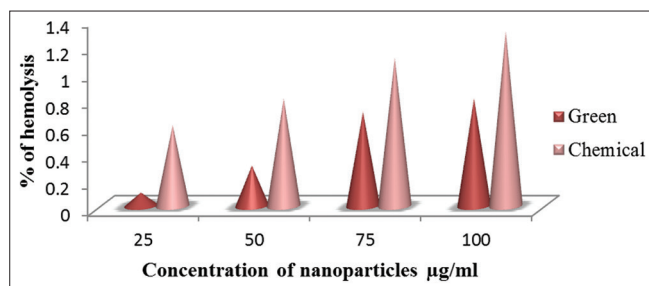


Fig. 10: Hemolysis activity of synthesized zinc oxide nanoparticles

biofilms and evaluated the effect of ZnONPs on biofilm formation, which is a major virulence factor of bacteria. The studies showed that well-developed biofilm formation by bacteria, whereas treatment with ZnONPs inhibited the biofilm formation in a dose-dependent manner. The percentage of hydrophobicity index was also decreased after treatment with ZnONPs compared to untreated bacteria [30]. In our present study too, among the two nanoparticles tested, green nanoparticles were able to inhibit the growth at lower concentration and time of exposure (12 h) and nearly complete inhibition at 72 h was noticed.

Hemolysis assay

To assess the toxicity of nanoparticles at the cellular level, hemolysis assay was performed. The hemolysis activity was done to gain additional information about the biocompatibility, for its *in vivo* applications. Erythrocyte is the most important component in the blood, so the nanoparticles interact with it. If cell lysis is <10%, it shows that there is no damage to the blood cells. It is mainly done to identify the lysis of the red blood cells. It was done using green and chemically synthesized ZnONPs.

Fig. 10 shows the plot of the percentage of hemolysis which increases with increase in concentration of nanoparticles ranging from 25 to 100 µg/ml. Among the two nanoparticles, the green synthesized nanoparticles showed the less hemolytic effect at all the concentrations, compared to chemically synthesized nanoparticles.

For different concentrations of zinc oxide, bulk materials of red blood cells (RBCs) were hemolyzed within 10–15 min of incubation, but in case of plant extract, no hemolysis occurred. In case of nanoparticles, hemolysis was observed at higher concentration after almost half an hour of incubation [17]. *Staphylococcal* α -hemolysin, a major virulence factor lysed the host cells by forming pores in the cell membrane. It showed that the addition of ZnONPs inhibited the RBC lysis caused by *S. aureus*. The addition of ZnONPs decreased the cell lysis and increased with increase in the concentration of ZnONPs. An important aspect of any therapeutic molecule is that the molecule should affect the function of a target molecule without harming the mammalian cells [30]. Hence, we have shown that ZnONPs have no cytotoxic effects of human blood cells.

Since it is necessary to develop environmental-friendly methods for the synthesis of nanoparticles, we opted for green synthesis. Hence, the green synthesized nanoparticle was found to be more effective in controlling the growth of microbes and also was found to be biocompatible. Hence, it can be exploited to treat the infections associated with microbial growth.

CONCLUSION

In the present study, we attempted to synthesis the ZnONPs by green and chemical methods. Both the nanoparticles were synthesized by coprecipitation method. The formation of ZnONPs was confirmed by UV-visible absorption spectroscopy. Characterization by FTIR and SEM analysis showed that the structure of synthesized ZnO nanoparticles to be spherical. XRD analysis further confirmed that the particles synthesized were crystalline in nature. Then, it was further analyzed for antimicrobial, cell viability, antibiofilm, and biocompatibility effect to

assess its biological application. Findings of our present study showed that the biocompatibility is good and hemolysis activity is less for green synthesized ZnONPs compared to chemically synthesized nanoparticles. The results showed that green synthesized nanoparticles have more inhibition activity as evident from the outcome of the antibacterial and antibiofilm activity.

AUTHORS' CONTRIBUTIONS

Experimentation and manuscript preparation were done by the authors V. Akhila and S. J. S. Banupriya. Formulation of the experimental design and the manuscript was edited by Dr. S. Sumathi and finally approved by the authors Dr. S. Sumathi and Dr. P. R. Padma.

CONFLICTS OF INTEREST

No conflicts of interest.

REFERENCES

1. Matinise N, Kaviyarasu K, Mongwaketi N, Khamlich S, Kotsedi L, Mayedwa M, et al. Green synthesis of novel Zinc iron oxide (ZnFe₂O₄) nanocomposite via *Moringa oleifera* natural extract for electrochemical applications. *Appl Surf Sci* 2018;446:66-73.
2. Manokari M, Ravindran CP, Shekhawat MS. Production of zinc oxide nanoparticles using aqueous extracts of a medicinal plant *Micrococca mercurialis* L. Benth. *World Sci News* 2016;30:117-28.
3. Cremonez CM, Leite FP, Bordon Kde C, Cerni FA, Cardoso IA, Gregório ZM, et al. Experimental *Lachesis muta rhombeata* envenomation and effects of soursop (*Annona muricata*) as natural antivenom. *J Venom Anim Toxins Incl Trop Dis* 2016;22:12.
4. Namasivayam SK, Prasanna M, Subathra S. Synergistic antibacterial activity of zinc oxide nanoparticles with antibiotics against the human pathogenic bacteria. *J Chem Pharm Res* 2015;7:133-8.
5. Perez C, Pauli M, Bazerque P. An antibiotic assay by Agar Well diffusion method. *Acta Biolo Med Exp* 1990;15:113-5.
6. Igarashi M, Miyazawa T. The growth inhibitory effect of conjugated linoleic acid on a human hepatoma cell line, HepG₂, is induced by a change in fatty acid metabolism, but not the facilitation of lipid peroxidation in the cells. *Biochim Biophys Acta* 2001;1530:162-71.
7. Christensen GD, Simpson WA, Younger JJ, Baddour LM, Barrett FF, Melton DM, et al. Adherence of coagulase-negative staphylococci to plastic tissue culture plates: A quantitative model for the adherence of staphylococci to medical devices. *J Clin Microbiol* 1985;22:996-1006.
8. Gleibs S, Mebs D, Werdning B. Studies on the origin and distribution of palytoxin in a Caribbean coral reef. *Toxicon* 1995;33:1531-7.
9. Parthiban C, Sundaramurthy N. Biosynthesis, characterization of zinc oxide nanoparticles by using *Pyrus pyrifolia* leaf extract and their photocatalytic activity. *Int J Innov Res Sci Eng Tech* 2015;4:9710-8.
10. Senthilkumar SR, Sivakumar T. Green tea (*Camellia sinensis*) mediated synthesis of Zinc oxide (ZnO) nanoparticles and studies on their antimicrobial activities. *Int J Pharm Pharm Sci* 2014;6:461-5.
11. Bagheri S, Chandrappa KG, Hamid SB. Facile synthesis of nano-sized ZnO by direct precipitation method. *Pharm Chem* 2014;5:265-70.
12. Hu D, Si W, Qin W, Jiao J, Li X, Gu X, et al. *Cucurbita pepo* leaf extract induced synthesis of zinc oxide nanoparticles, characterization for the treatment of femoral fracture. *J Photochem Photobiol B* 2019;195:12-6.
13. Raj LF, Jayalakshmy E. Biosynthesis and characterization of Zinc oxide nanoparticles using root extract of *Zingiber officinale*. *Orient J Chem* 2015;31:51-6.
14. Prakash MJ, Kalayanasundharam S. Biosynthesis, characterization, free radical scavenging activity and anti-bacterial effect of plant mediated Zinc oxide nanoparticles using *Pithecellobium dulce* and *Lagenaria siceraria* leaf extracts. *Int J Nano Mater Sci* 2015;4:55-69.
15. Kunasekaran V, Krishnamoorthy K. Compatible studies of rasagiline mesylate with selected excipients for an effective solid lipid nanoparticles formulation. *Int J Pharm Pharm Sci* 2015;7:73-80.
16. Ramesh P, Rajendran A, Subramanian A. Synthesis of zinc oxide nanoparticles from fruits of *Citrus aurantifolia* by chemical and green method. *Asian J Phytomed Clin Res* 2014;2:189-95.
17. Gnanasangeetha D, Thambavani SD. Facile and eco-friendly method for the synthesis of Zinc oxide nanoparticles using *Azadirachta* and *Emblica*. *Int J Pharm Sci Res* 2014;5:2866-73.
18. Ibrahimel-Assal M, Menofy NG. Chitosan nanoparticles as drug delivery system for cephalixin and its antimicrobial activity against multidrug resistant bacteria. *Int J Pharm Pharm Sci* 2019;7:14-27.

19. Yadav R, Bandopadhyay M, Saha A, Mandal AK. Synthesis, characterisation, antibacterial and cytotoxic assays of zinc oxide (ZnO) nanoparticles. *Br Biotechnol J* 2014;9:1-10.
20. Bhumi G, Savithamma N. Biological synthesis of zinc oxide nanoparticles from *Catharanthus roseus* (L.) G. Don. leaf extract and validation for antibacterial activity. *Int J Drug Dev Res* 2014;6:208-14.
21. Ratney YJ, David SB. Antibacterial activity of zinc oxide nanoparticles by sonochemical method and green method using *Zingiber officinale*. *Green Chem Tech Lett* 2016;2:11-5.
22. Abdel-Aziem A. An efficient and simple synthesis 2, 3-Dihydro-1, 3, 4-Thiadiazoles, pyrazoles and coumarins containing benzofuran moiety using both conventional and grinding methods. *Int J Pharm Pharm Sci* 2015;7:61-8.
23. Shankar S, Rhim J. Effect of Zn salts and hydrolyzing agents on the morphology and antibacterial activity of zinc oxide nanoparticles. *Environ Chem Lett* 2019;17:1105-9.
24. Barkhordari A, Hekmatimoghaddam S, Jebali A, Khalili MA, Talebi A, Noorani M, et al. Effect of zinc oxide nanoparticles on viability of human spermatozoa. *Iran J Reprod Med* 2013;11:767-71.
25. Fakhroueian Z, Deshiri AM, Katouzian F, Esmailzadeh P. *In vitro* cytotoxic effects of modified zinc oxide quantum dots on breast cancer cell lines (MCF7), colon cancer cell lines (HT29) and various fungi. *J Nanopart Res* 2014;5:1-14.
26. Fazio E, Santoro M, Franco MS, Guglielmino PP, Neri F. Iron oxide nanoparticles prepared by laser ablation: Synthesis, structural properties and antimicrobial activity. *Collids Surf A* 2016;490:98-103.
27. Alijani HQ, Pourseyedi S, Torkzadeh-Mahani M, Khatami M. Green synthesis of zinc sulfide (ZnS) nanoparticles using *Stevia rebaudiana* Bertoni and evaluation of its cytotoxic properties. *J Mol Struct* 2018;1175:214-218.
28. Hussain A, Oves M, Alajmi MF, Hussain I, Amir S, Ahmed J, et al. Biogenesis of ZnO nanoparticles using *Pandanus odorifer* leaf extract: Anticancer and antimicrobial activities. *RSC Adv* 2019;9:15357-70.
29. Khan ST, Ahmad J, Ahamed M, Musarrat J, Al-Khedhairi AA. Zinc oxide and titanium dioxide nanoparticles induce oxidative stress, inhibit growth, and attenuate biofilm formation activity of *Streptococcus mitis*. *J Biol Inorg Chem* 2016;21:295-303.
30. Pati R, Mehta RK, Mohanty S, Padhi A, Sengupta M, Vaseeharan B, et al. Topical application of zinc oxide nanoparticles reduces bacterial skin infection in mice and exhibits antibacterial activity by inducing oxidative stress response and cell membrane disintegration in macrophages. *Nanomedicine* 2014;10:1195-208.